Plasma Chem Plasma Process (2007) 27:225–240
DOI 10.1007/s11090-007-9057-3

ORIGINAL PAPER

Influence of the Excited States of Atomic Nitrogen $N(^2D)$, $N(^2P)$ and N(R) on the Transport Properties of Nitrogen. Part II: Nitrogen Plasma Properties

B. Sourd · P. André · J. Aubreton · M.-F. Elchinger

Received: 11 December 2006 / Accepted: 25 January 2007 / Published online: 16 March 2007

Abstract In this paper, the calculated values of the viscosity and thermal conductivity of nitrogen plasma are presented taking into account five (e, N, N^+, N_2 and N_2^+) or eight (e, $N(^4S)$, $N(^2P)$, $N(^2D)$, N(R), N^+, N_2 and N_2^+) species. The calculations are based on the supposition that the temperature dependent probability of occupation of the states is given by the Boltzmann factor. The domain for which the calculations are performed, is for $p = 1$ and 10 atm in the temperature range from 5,000 K to 15,000 K. Classical collision integrals are used in calculating the transport coefficients and we have introduced new averaged collision integrals where the weight associated at each interacting species pair is the probable collision frequency. The influence of the collision integral values and energy transfer between two different species is studied. These results are compared which those of published theoretical studies.

Keywords Transport coefficients · Transport properties · Viscosity · Thermal conductivity · Nitrogen · Plasma

Introduction

Transport properties of thermal plasmas have been calculated by many authors due to their importance in many technological applications [1, 2]. But recently, Capitelli et al. [3, 4] have studied the dependence of transport coefficients (thermal conductivity, viscosity, electrical conductivity), on the presence of electronically atomic excited states H(n), in LTE H_2 plasmas. They deduce that excited states with their ''abnormal'' cross sections strongly influence the transport coefficient especially at high pressure. They also showed

B. Sourd · J. Aubreton · M.-F. Elchinger (✉)
SPCTS University of Limoges, 123 Av. A. Thomas, 87060 Limoges cedex, France
e-mail: marie.elchinger@unilim.fr

P. André
LAEPT Blaise Pascal University, 24 av. des Landais, 63177 Aubiere cedex, France

the effect of excited states on the transport of ionization energy in thermal plasmas in the temperature range of 10,000–25,000 K, taking into account the dependence of diffusion cross sections on principal quantum number [5]. Their results show a strong effect due to excited states at high pressure while compensation effects reduce their role at atmospheric pressure. These authors [6] also calculated resonant charge—exchange cross sections and the relevant transport (diffusion) cross sections for excited states of nitrogen and oxygen atoms.

The aim of our work is to study the influence of the excited states of atomic nitrogen on the transport properties of two e/N mixtures in the temperature range of 5,000–15,000 K and at two pressure values (p = 1 and 10 atm). The first mixture takes into account five gaseous species : e, N, N^+, N_2 and N_2^+, the second system eight species : e, N(^{4}S), N(^{2}P), N(^{2}D), N(R), N^+, N_2 and N_2^+ where ''R'' represents the excited states of monoatomic nitrogen different of (^{2}P) and (^{2}D). In the first part of the paper, the plasma composition and the different potentials, permitting to describe all collisions are calculated. The second part is devoted to calculation of transport properties in two cases, with and without consideration of energy transfer between the excited states of N.

Calculation of the Plasma Composition

To determine the composition of the plasma, the classical method consists of minimizing the Gibbs free energy under mass and charge conservation constraints. The minimization is achieved by using Lagrange's multipliers and the solution of the corresponding set of equations is based on the steepest descent method according to White and Dantzig [7]. For (e, N^+, N_2 and N_2^+) species we have used the same thermodynamic data but the data used for N is summarized in Table 1:

In Table 1 Q_{int} is the internal partition function, ΔH_{f0}^0 is the enthalpy of the chemical species related to an absolute reference state (T = 0 K) and the energy attributed to a state X is obtained as:

$$E_X = \sum_i g_{x,i} \times E_{x,i}$$

where $g_{x,i}$ is the statistical weight (as an example for state ^{2}D we have $g_{D,1} = 6$ and $g_{D,2} = 4$) and $E_{x,i}$ is energy (as an example for state ^{2}D we have $E_{D,1} = 19224.46\ \ cm^{-1}$ and $E_{D,2} = 19233.18\ \ cm^{-1}$). For calculation of the partition function the summation is limited due to the lowering of ionization energy ΔE_i (Debye Hückel approach) which depends on electronic density.

The Fig. 1 shows the evolution with temperature of the density of species at p = 1 atm for a nitrogen plasma calculated for the two different retained species (five or eight).

Table 1 Data used for N

	N	N(^{4}S)	N(^{2}D)	N(^{2}P)	N(R)
Q_{int}	$\sum_{i=1} g_i \exp\left(-\frac{E_i}{kT}\right)$	4	10	6	$\sum_{i=4} g_i \exp\left(-\frac{E_i - E_4}{kT}\right)$
E_i (cm^{-1})	0	0	19,228	28,839	83,336
ΔH_{f0}^0 ($kJ.mol^{-1}$)	470.82	470.82	700.84	815.81	1467.74

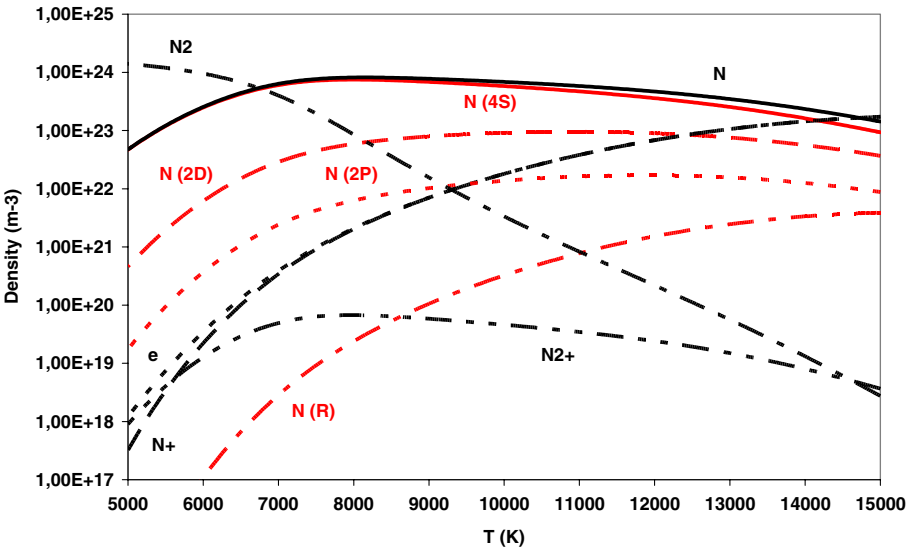

Fig. 1 Evolution of density versus temperature (p = 1 atm)

We have obtained the same values for the densities, at a given temperature, independent of the number of species taken into account. Moreover we have $n(N) = n(N(^4S)) + n(N(^2D)) + n(N(^2P)) + n(N(R))$. The relative discrepancy is always less than 0.001% of the absolute values for all the densities. In Fig. 2 the same kind of calculation is done with p = 10 atm.

At 15,000 K, the values of the ratio $n(R)/n(N) \equiv Q(R)/Q(N)$ are respectively 0.027 and 0.012 for p = 1 atm and 10 atm. In this case the contribution of the R states is greater than (for the same temperature) for p = 1 atm. The result may be explained by the fact that:

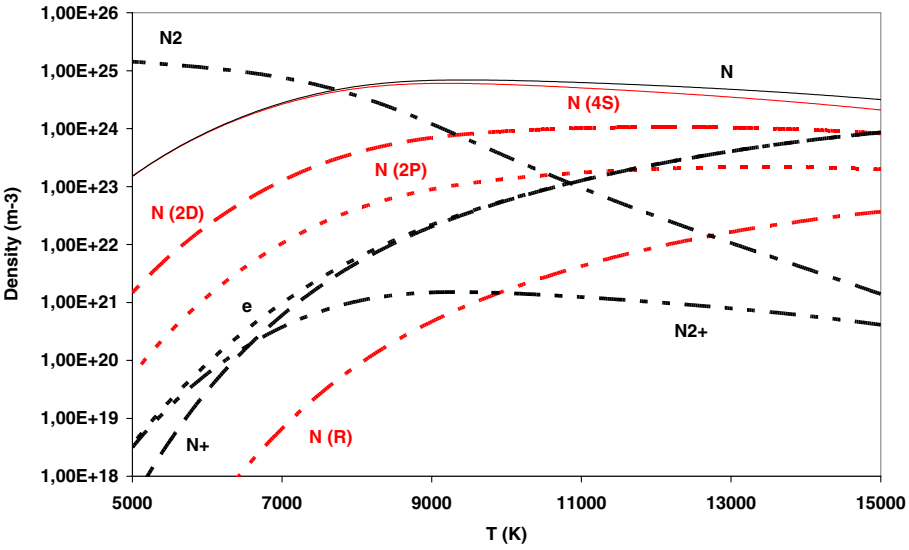

Fig. 2 Evolution of density versus temperature (p = 10 atm)

– Q(R) is more influenced than Q(N) by the limitation theory (lowering ionization energy),
– The electronic density is higher for p = 10 atm (respectively $n_e = 1.724 \times 10^{23}$ m^{-3} and 8.581×10^{23} m^{-3} for p = 1 and 10 atm) leading to ΔE_i (10 atm) $> \Delta E_i$ (1 atm).

Collision Integrals

Collision integrals (noted $\bar{Q}_{i,j}^{(\ell,s)}$) are required to calculate transport coefficients and account for the interaction between colliding species i and j: in our conditions of pressure only binary collisions between all the species are considered. The indices (ℓ, s) are directly related to the order of the approximation used for the transport coefficients: viscosity, electrical conductivity, translational and reactional thermal conductivities are calculated at the third approximation and internal thermal conductivity is obtained at the first approximation [8–10]. A previous study [9] has shown that all combinations of numbers (ℓ, s) have to be calculated for $\bar{Q}_{i,j}^{(\ell,s)}$ up to $\ell_{max} = 3$ and $s_{max} = 5$, provided $\ell \leq s$.

The transport cross sections $Q_{i,j}^{(\ell)}$ are determined from internuclear interaction potential, quantum approach and directly by numerical integration of differential cross sections. All these different methods are presented elsewhere: section 2 [11]. In Table 2 we give all the binary interactions taken into account for the five species mixture.

In Table 2 the data is taken from one of our previous papers [9, 11, 12] where the collision integrals are calculated, P and • refer to a polarizability potential (the dipolar polarizability of N_2 is 1.7301 $Å^3$ [13] leading to $V_{N2p} = 12.456$ eV $Å^4$, same notations as [11]) and to unknown interactions respectively, which are to be determined in this study. Now, the three following interactions are studied: N_2–N_2 and N–N_2 and e–N_2.

N_2–N_2 Interaction

Accurate collision integrals are available in Stallcop et al. [14] but our formalism needs three more integrals ($\bar{Q}^{(2,5)}$, $\bar{Q}^{(3,4)}$ and $\bar{Q}^{(3,5)}$) and also for T > 10,000 K. Therefore we had to determine a new set of collision integrals and for that we used the data given by Stallcop et al. [14, 15] to create an effective potential. The obtained values are fitted by non-linear regression to calculate the three Hulburt–Hirschfelder potential parameters [11]:

$$D_e = 0.0117\,\text{eV} \text{ and } r_m = 3.995\,Å$$
$$\alpha = 6.6842, \beta = 2.0202 \text{ and } \gamma = 0.5705.$$

Table 2 Interactions taken into account

	e	N	N^+	N_2	N_2^+
e	(9)	(11)	(9)	•	(9)
N		(11, 12)	(11)	•	(11)
N^+			(9)	P	(9)
N_2				•	P
N_2^+					(9)

where D_e and r_e are respectively the depth of the potential well and the position of the minimum of the potential well.

Finally, our results are in very good agreement with those of Stallcop et al. [14] (the relative discrepancy is less than 3% on all the temperature range for $T \geq 300$ K and independent of the collision integrals). As an example, we obtain $\bar{Q}^{(2,2)} = 43.10$ and 22.45 10^{-20} m^2, for T = 300 and 10,000 K, to be compare to 43.08 and 22.98 10^{-20} m^2 [14].

$N–N_2$ Interaction

For this interaction, we have the same problem that for the N_2 – N_2 collision [16]. Therefore we used the effective potential energy of Stallcop et al. [16] determined from the θ_0 orientation which yields accurate transport data with a little computational effort (the angle θ_0 satisfies $P_2(\cos\theta_0) = 0$ where P_2 is a zero-order Legendre polynomial of degree 2, i.e., $\theta_0 = 54.73561^\circ$). The Hulburt–Hirschfelder potential parameters are the following:

$$D_e = 0.00776\,\text{eV} \text{ and } r_m = 3.742\,\text{Å}.$$
$$\alpha = 7.0095, \beta = 12.6825 \text{ and } \gamma = 1.1696.$$

As for N_2–N_2 interaction our results are in very good agreement with those of Stallcop et al. [16] (the relative discrepancy is less than 2% on all the temperature range for $T \geq 300$ K independent of the collision integrals).

$e–N_2$ Interaction

For e–N_2 interaction we split up the energy range into three parts: ε<1.5 eV, 1.5 eV $\leq \varepsilon \leq$ 4 eV and ε>4 eV

Energy below Resonance Region (ε<1.5 eV)

Theoretical and experimental analysis of low-energy electron-N_2 scattering has been done by Sun et al. [17]

- We have used their experimental results, for three energy values: $\varepsilon = 0.55$, 1.0 and 1.5 eV, for the differential elastic cross-sections at scattering angles from 20° to 130° completed for the small and large angles.
- For lower energies (ε<0.55 eV) we have no experimental or theoretical data for differential elastic cross-sections but we have only the values of the total elastic cross sections $Q_T(\varepsilon)$ down to $\varepsilon = 0.08$ eV and 0.02 eV (respectively for experimental and theoretical approaches). For our calculations we started from $Q_T(\varepsilon)$ and we retained:

– For 0.08<ε<0.35 eV the experimental values
– For 0.02<ε<0.08 eV the theoretical values and we assume that experimental are the same (Sun et al. [17]: Table 9).

Then we calculated the transfer cross sections $Q^{(\ell)}$. For that, we started from general formalism of the elastic scattering cross sections which may be written as [18]:

$$Q_j^k(\varepsilon) = 2\pi \int_0^{\pi} \sigma^k(\varepsilon,\theta) P_j(\cos\theta)\sin\theta d\theta \tag{1}$$

where $\sigma^k(\varepsilon,\theta)$ is a differential cross section for electron scattering through an angle θ for process k. Therefore,$Q_0^0(\varepsilon)$, the total elastic cross section, is written as:

$$Q_T(\varepsilon) = Q_0^0(\varepsilon) = 2\pi \int_0^{\pi} \sigma^0(\varepsilon,\theta)\sin\theta d\theta \quad (P_0 = 1) \tag{2}$$

By using the relation (1) and the expressions of Legendre polynomial we obtained the following equations for the transfer cross sections:

$$Q^{(1)}(\varepsilon) = Q_0^0(\varepsilon)\left(1 - R_0^1(\varepsilon)\right) \quad \text{with} \quad R_0^1(\varepsilon) = \frac{Q_1^0(\varepsilon)}{Q_0^0(\varepsilon)} \tag{3}$$

$$Q^{(2)}(\varepsilon) = \tfrac{2}{3} Q_0^0(\varepsilon)\left(1 - R_0^2(\varepsilon)\right) \quad \text{with} \quad R_0^2(\varepsilon) = \frac{Q_2^0(\varepsilon)}{Q_0^0(\varepsilon)} \tag{4}$$

$$Q^{(3)}(\varepsilon) = Q_0^0(\varepsilon)\left(1 - \tfrac{3}{5} R_0^1(\varepsilon) - \tfrac{2}{5} R_0^3(\varepsilon)\right) \quad \text{with} \quad R_0^3(\varepsilon) = \frac{Q_3^0(\varepsilon)}{Q_0^0(\varepsilon)} \tag{5}$$

We know $Q_0^0(\varepsilon)$ but it is necessary to determine $R_0^i(\varepsilon) i \in [1,3]$, leading to $Q^{(1)}(\varepsilon),\ldots,Q^{(3)}(\varepsilon)$, by extrapolation.

To calculate $R_0^i(\varepsilon)$, $i \in [1,3]$, we have used obtained results at 0.55 eV, 1.0 eV and 1.5 eV. For these energy values, we have $Q_0^0(\varepsilon)$ and $Q^{(i)}(\varepsilon), i \in [1,3]$ that leads to:

$$R_0^1 = 1 - \frac{Q^{(1)}}{Q_0^0};\ R_0^2 = 1 - \frac{3}{2}\frac{Q^{(2)}}{Q_0^0} \text{ and } R_0^3 = \frac{5}{2}\left(1 - \frac{3}{5} R_0^1 - \frac{Q^{(3)}}{Q_0^0}\right)$$

and the values calculated from above are tabulated in Table 3:

For this extrapolation at low energy we used a simple polynomial (three coefficients) form expressed as:

$$R_0^i(\varepsilon) = a\varepsilon + b\varepsilon^2 + c\varepsilon^3$$

This choice is justified by the fact that $R_0^i(0) = 0$: when ε is closed to zero i.e., the series of quantum phase shifts is reduced to its first term and we have $Q^{(1)} = Q^{(3)} = Q_T$ and $Q^{(2)} = \frac{2}{3} Q_T$. This approach leads to realistic results for R_0^2 and R_0^3 but not for R_0^1 further we noticed that the contribution of R_0^3 is low in the given energy range. Then according to the works of Phelps [18], we have improved the analytic form for R_0^1 :

Table 3 Values of the parameters R_0^i (ε) of Legendre polynomial for the considered energies (ε)

ε (eV)	R_0^1	R_0^2	R_0^3
0.55	−0.1537	−0.0587	−0.0013
1.0	−0.0975	−0.1006	−0.0095
1.5	−0.0307	−0.1403	−0.0078

$$R_0^1 = \frac{\varepsilon(a + b\varepsilon)}{1 + c\varepsilon + d\varepsilon^2}$$

To determine the fourth coefficient we have imposed, by a graphical study, $R_0^1 = 0$ for $\varepsilon = 1.80$ eV.

To conclude, using known $Q_T(\varepsilon)$ and R_0^i for $i \in [1,3]$, we have determined $Q^{(\ell)}(\varepsilon)$ for $\ell \in [1,3]$ in the energy range 0.02–0.55 eV.

For Resonant Energies (1.5 eV ≤ ε ≤ 4.0 eV)

In this energy range, resonant diffusions (for example, the π_g resonance for $\varepsilon \sim 2.4$ eV) appear that introduce oscillations in the vibrationally elastic ($0 \rightarrow 0$) and inelastic ($0 \rightarrow v$) cross sections. First, we calculated the elastic cross sections ($Q^{(i)}(\varepsilon)$, $i \in [1,3]$) for the four following values of energy: $\varepsilon = 1.92$, 1.98, 2.46 and 2.605 eV [17]. And then we determined the resonant shape based on the works of Sun et al. [17] (experimental energy dependence of differential cross sections at a scattering angle of 60°) and Shyn et al. [19], the values of $Q^{(i)}$ were obtained in this energy range using proportionality's rules.

Energy above the Resonant Region (ε>4.0 eV)

- For 4 eV ≤ ε ≤ 10 eV: we used the experimental results of Sun et al. [17] and applied it further for low energies, small angles and large angles.
- For $\varepsilon = 24.5$ eV, we retained the experimental results of Mi et al. [20]
- For higher energy (up to 400 eV) we have used the results of Shyn et al. [19] that allowed us to complement the previous data.

Conclusion. Collision integrals

So we have all collision integrals for the first (five species) system while for (eight species) system had to do some assumptions.

– Firstly we consider that the following collisions $X - N(^4S)$, $X - N(^2D)$, $X - N(^2P)$ and $X - N(R)$ with X = e, N^+, N_2 and N_2^+, are equivalent to X–N (see Table 2). For the three collisions $N(^4S, ^2D, ^2P) - N^+(^3P)$, Eletskii et al. [6] showed that they are quite similar. In addition to the ones mentioned they took into account high electronically excited states of $N(ns(^2P,^4P))$ and the ground state of $N^+(^3P)$ while completely neglected the other states: $^2S^\circ$, $^2D^\circ$ ... for N and ^1D, ^1S, ... for N^+.
– Secondly in Table 4 we give only the binary interactions between the different atomic nitrogen species. The number gives the reference number of the first paper and as the potential interactions of some collisions are unknown we also present the equivalent collision integrals taken into account.

Table 4 Interactions taking into account

	$N(^4S)$	$N(^2D)$	$N(^2P)$	N(R)
$N(^4S)$	(12)	(12)	(12)	^4S–^2D
$N(^2D)$		(12)	(12)	^4S–^2D
$N(^2P)$			^2D–^2D	^4S–^2D
N(R)				^2D–^2D

For the interactions $N(^4S)$–$N(^2P)$ and $N(^2D)$–$N(^2P)$:

- For $\ell = 2$ the integral collisions are calculated starting from the known interaction potentials,
- For $\ell = 1$, 3 we introduce the transfer integral collisions of the interactions $N(^4S)$–$N(^2D)$.

Results

We have done three types of calculations for the transport properties (as in part I), for the first two were for five species chemical system and the last dealt with eight species chemical system:

(a) It is the usual case, the collision integrals are determined only with the $N(^4S)$–$N(^4S)$ interaction and we write down our results in ''SS'',

(b) As in part I (section 'e–N_2 interaction'), we have generalized the weighted collision integrals by introducing the probability α associated with two interacting species i and j (i, j = S, D, P or R for $N(^4S)$, $N(^2D)$, $N(^2P)$ or N(R) respectively) as $\alpha_{ij} = \frac{n(i)}{n(N)} \times \frac{n(j)}{n(N)}$ (independent probability hypothesis) and we have verified that $\sum_{i,j} \alpha_{ij} = 1$. But as N(R) is dependent on composition and we have to calculate $\bar{Q}_f^{(\ell,s)}$ directly in the computer code and we denoted our results ''wgh''.

(c) In this case (eight species), $N(^4S)$, $N(^2D)$, $N(^2P)$ and N(R) are considered as independent chemical species, then the transport properties are determined classically and ours results are noted ''SDPR''.

To calculate the transport properties classical Cramer's rule can be used i.e., the solution of a set of linear equations can be expressed as the ratio of determinants. Another way is to solve directly the set of linear equations. The viscosity can be expressed as:

$$\eta(\xi) = \frac{1}{2} kT \sum n_j b_{jo}(\xi) = \sum_j \eta_j(\xi) \tag{6}$$

where $\eta_j(\xi) = \frac{1}{2} kTn b_{jo}(\xi)$ is the viscosity of j specie at ξ order of approximation (in this paper ξ = 3): equation 7.4–20 [21]. We have the same kind of results for translational thermal conductivity: $k_{tr}(\xi) = \sum_j k_{tr}^j$. Now we present some results of thermal conductivity and viscosity for the two values of the pressure (p = 1 and 10 atm).

Thermal Conductivity

Figure 3 shows the evolution of translational thermal conductivity versus temperature at p = 1 atm obtained by the three calculation methods. Here $k_{tr}(SDPR) = k(^4S) + k_{tr}(^2D) + k(^2P) + k_{tr}(R)$ where $k_{tr}(X)$ is the translational thermal conductivity associated at the specie X.

The shape of k_{tr} (SDPR), k_{tr} (SS) and k_{tr} (wgh) follows the temperature evolution of n(N) and $n(N(^4S))$ i.e., the numerical densities of these species are smaller than $n(N_2)$ at

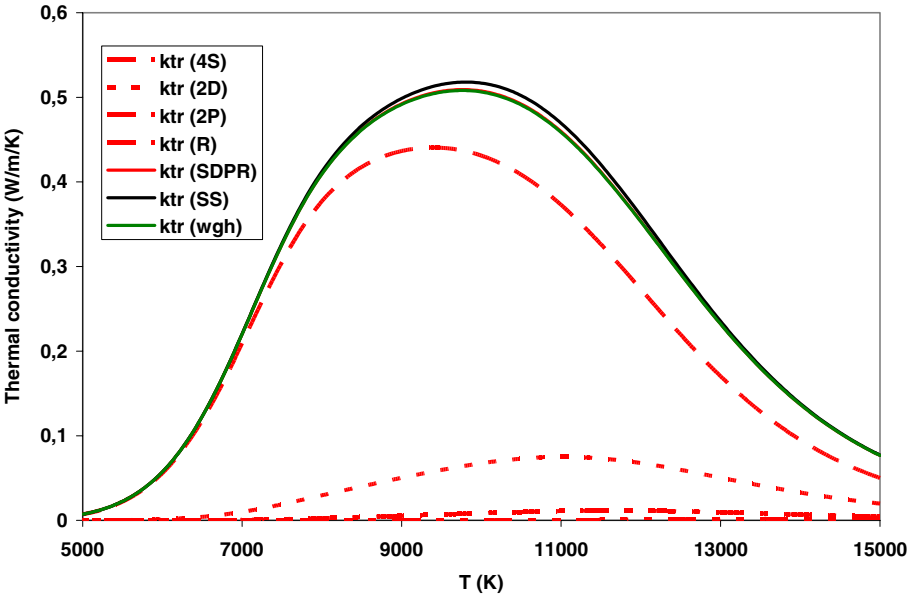

Fig. 3 Evolution of the translational thermal conductivity as function of temperature (p = 1 atm)

T = 5,000 K and $n(N^+)$ at T = 15,000 K, the molar fractions x(N) and $x(N(^4S))$ are maximum at around T = 9,500 K. As shown in part I, the contribution of each state to the total translational thermal conductivity has been determined, for T < 7,000 K, we have $k(SDPR) = k_{tr}(^4S) = k(SS) = k_{tr}(wgh)$. With the increase temperature the excited states play a more important role but $k_{tr}(^2P)$ and k_{tr} (R) remain negligible (their numerical densities are small in the temperature range) and only $k_{tr}(^2D)$ contributed notably to $k_{tr}(SDPR)$. For T = 11,000 K we have $k_{tr}(^2D)$ = 0.075 $Wm^{-1}K^{-1}$ and k_{tr} (SDPR) = 0.459 $Wm^{-1}K^{-1}$, leading to relative contribution of 16% (82% for $k_{tr}(^4S)$ and 2% for the two other states).

As previously remarked the transfer of energy between the different states of N leads to small variations on the values of the translational thermal conductivity. We have k (SDPR) $\approx k_{tr}$ (wgh), and the maximum relative discrepancy between k_{tr} (SDPR) and k_{tr} (SS) is obtained around 10,000 K and which, for all the temperature values in the range, the discrepancy is even less 3%. Finally, at T = 15,000 K we have k_{tr} (SDPR) $\approx k_{tr}$ (wgh) $\approx$ k (SS), for this temperature N–N^+ and N^+–N^+ interactions (the integral collisions are the same whatever the calculation method) play an important role on transport properties.

For p = 1 atm, the temperature where the two different approaches lead to discrepancies between transport properties, is around 10,000 K. Figure 4 depicts the dependence on temperature, p = 1 atm, of internal (k_{int}) and reaction (k_{reac}) thermal conductivities. The total thermal conductivity k_t is the sum of the internal and reaction conductivities.

In this temperature range we have:

- $k_{int}(SDPR) \approx 0$ then $k_{reac}(SDPR) \approx k_t(SDPR)$,
- $k_{reac}(SS) \approx k_{reac}(wgh)$, these two transport properties take into account the dissociation ($N_2 \rightarrow 2N$ at low temperature) and ionization ($N \rightarrow N^+ + e$ at high temperature) reactions. Thence, on Fig. 4, we have omitted $k_{int}(SDPR)$ and $k_{reac}(wgh)$.

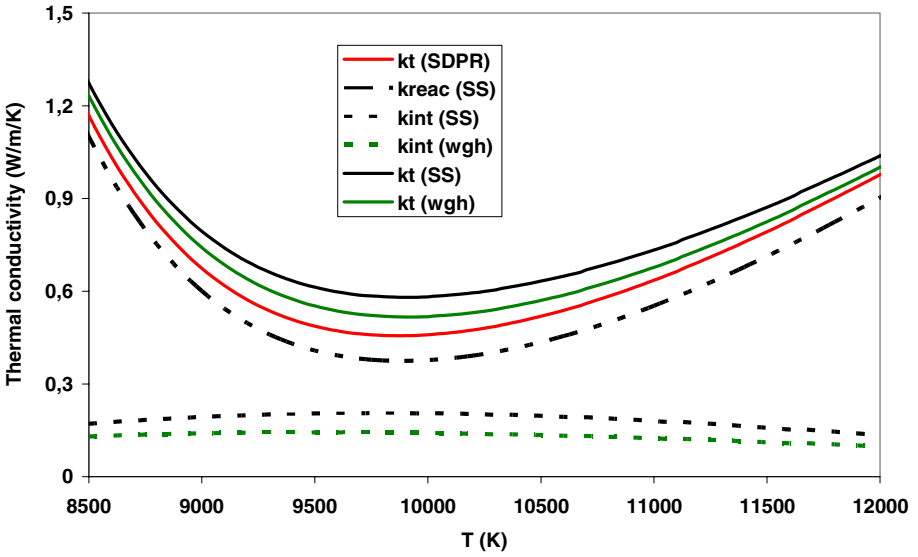

Fig. 4 Evolution of the thermal conductivities (p = 1 atm)

As usual, for p = 1 atm, the minimum values for k_t is around 10,000 K. For this temperature value we have k_t(SDPR) = 0.459, k_t(SS) = 0.582 and k_t(wgh) = 0.518 $Wm^{-1}K^{-1}$, leading to relative discrepancies (k_t(SS) is taken as the reference) of 21% (SDPR) and 11% (wgh). It should be noted that k_t(wgh) $\approx$ k_t(SS) at low temperature (T = 8,500 K) and k_t(wgh) $\approx$ k_t(SDPR) at high temperature (T = 12,000 K): the excited states influence on the determination of the averaged collision integrals $\bar{Q}_f^{(\ell,s)}$.

On Figs. 5 and 6, we show the evolution of the total thermal conductivity versus temperature (8,500 < T < 12,000 K for p = 1 atm and 9,500 < T < 13,000 K for p = 10 atm).

The introduction of the translational thermal conductivity shifts the minimum of k_{tot} to a lower temperature: 9,500 K against 10,000 K. Now for this temperature we have k (SDPR) = 1.271, k_{tot} (SS) = 1.406 and k_{tot} (wgh) = 1.336 $Wm^{-1}K^{-1}$. Remark that k_{tot} (SDPR)–k_{tot} (SS) = 0.135 $Wm^{-1}K^{-1}$ compared to 0.123 $Wm^{-1}K^{-1}$ obtained previously for k_t(SDPR)–k_t(SS) at 10000 K. This is due to the small influence of transfer collision integrals on translational thermal conductivity. The relative discrepancies (k_t(SS) is always taken as the reference) are of 10% for (SDPR) and 5% for (wgh). The same explanation for the relative position of k_{tot} (wgh) is valid in this case as well.

To emphasize the influence of the excited states on the transport properties we have increased the pressure up to 10 atm. As expected the minimum of the total thermal conductivity is shifted at higher temperature: 11,000 K against 9,500 K. Now for this temperature we have k_{tot} (SDPR) = 1.631, k_{tot} (SS) = 1.789 and k_{tot} (wgh) = 1.688 $Wm^{-1}K^{-1}$. Remark that k_{tot} (SDPR)–k_{tot} (SS) = 0.158 $Wm^{-1}K^{-1}$ compared to 0.135 $Wm^{-1}K^{-1}$ obtained previously for k_{tot} (SDPR) –k (SS) at 9,500 K, this increase is due to the influence of excited states of N. However, the relative discrepancies (k_t(SS) is always taken as the reference) are quite the same and we have 9% and 3% for (SDPR) and (wgh) respectively. The same explanation is valid for the relative position of k (wgh) as well.

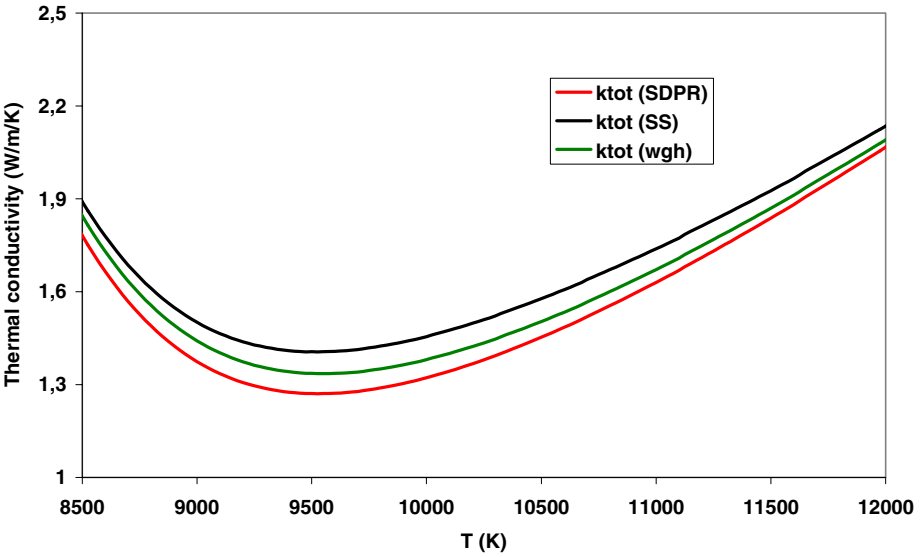

Fig. 5 Evolution of the total thermal conductivities (p = 1 atm)

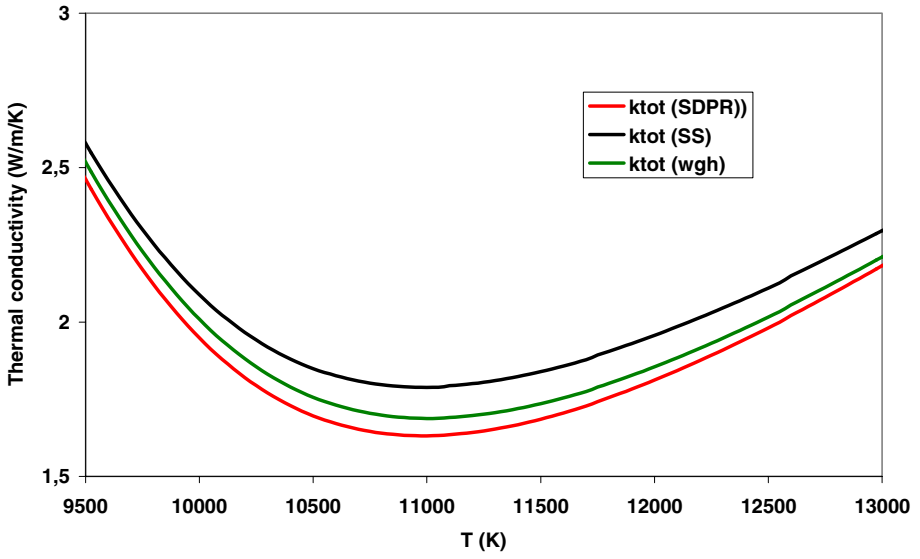

Fig. 6 Evolution of the total thermal conductivities (p = 10 atm)

Viscosity

Figures 7 and 8 show the evolution of the total viscosity versus temperature (7,500 < T < 12,000 K for p = 1 atm and 9,000 < T < 14,000 K for p = 10 atm). As remarked in part I we have $\mu(\text{wgh}) \approx \mu$ (SDPR) independent temperature and pressure values. The collision

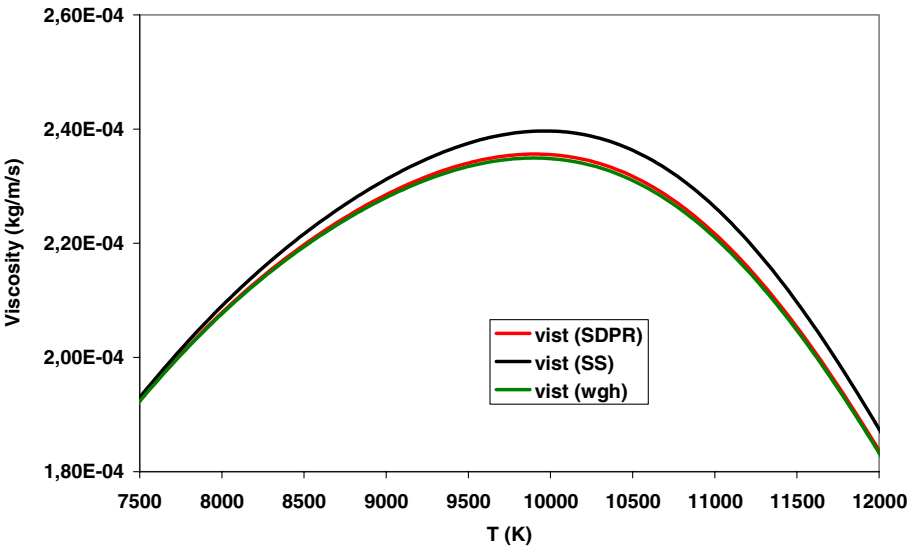

Fig. 7 Evolution of the total viscosity (p = 1 atm)

integrals (ℓ = 1 and 3) are strongly influenced by energy transfer between excited species involved only in the viscosity correction i.e., for a pure gas we have $\mu = f\left(\bar{Q}^{(2,2)}\right)$.

The maximum discrepancy (corresponding to the maximum values of the viscosity), obtained at T $\approx$ 10,000 K, between μ(SS) $=2.397 \times 10^{-4}$ $\mathrm{kgm^{-1}s^{-1}}$ and μ(SDPR) $=2.355 \times 10^{-4}$ $\mathrm{kgm^{-1}s^{-1}}$ is $\Delta\mu$ = 0.042 $\mathrm{kgm^{-1}s^{-1}}$, that is a relative discrepancy of 2%. In Table 5 we report the total viscosity along with the viscosity contributions (in 10^{-4} $\mathrm{kgm^{-1}s^{-1}}$) of N(^{4}S), N(^{2}D), N^+ and N_2 for different temperatures.

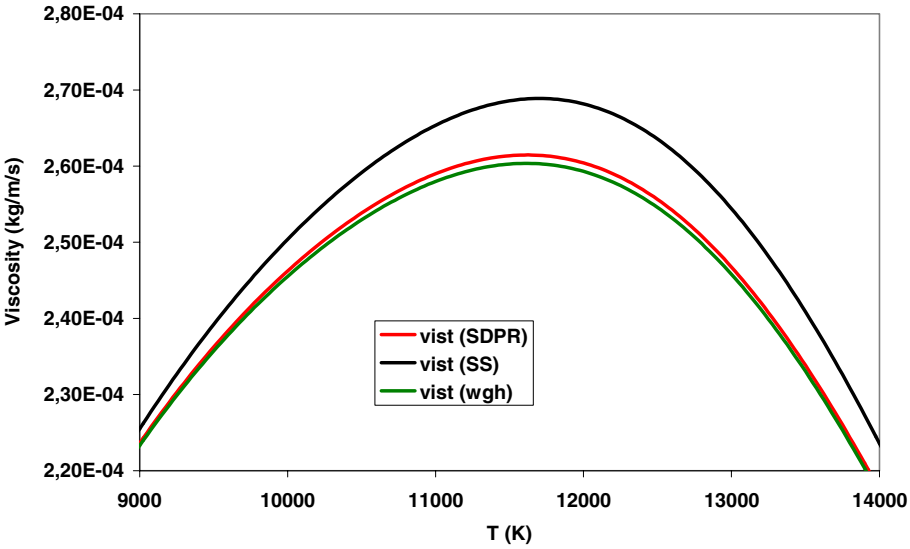

Fig. 8 Evolution of the total viscosity (p = 10 atm)

Table 5 Viscosity values for p = 1 atm

T (K)	N(^{4}S)	N(^{2}D)	N^+	N_2	N(^{4}S)...N_2	Total
8,000	1.694	0.133	0.004	0.237	2.068	2.079
10,000	1.960	0.307	0.037	0.015	2.319	2.355
12,000	1.349	0.334	0.094	0.001	1.778	1.837

In Table 5 N(^{4}S)...N_2 represents the sum of the four contributions. The difference between the values of these sums and μ_T is principally due to N(^{2}P) contribution which is 0.054×10^{-4} kgm^{-1}s^{-1} at 12,000 K. In temperature range (8,000–12,000 K) the main contribution to μ_T is μ (N(^{4}S)): between 70 and 80%.

For Fig. 8 (p = 10 atm) can be explained in the same way as Fig. 7 (p = 1atm). In this case the maximum value of viscosity is obtained for T $\approx$ 11,700 K and for this temperature value we have μ(SS) =2.689×10^{-4} kgm^{-1}s^{-1} and μ(SDPR) =2.614×10^{-4} kgm^{-1}s^{-1} leading to $\Delta\mu$ = 0.075 kgm^{-1}s^{-1} and a relative discrepancy of 3%.

Discussion and Conclusion

In these two papers we have tested the influence of the excited states of N on the transport properties (thermal conductivity and viscosity). In the first part we have taken into account only three species (N(^{4}S), N(^{2}D) and N(^{2}P)) and introduced new averaged collision integral $\bar{Q}_f$. In the second part we have taken into account five (e, N, N^+, N_2 and N_2^+) or eight (e, N(^{4}S), N(^{2}P), N(^{2}D), N(R), N^+, N_2 and N_2^+) species and we have generalized the weighted collision integrals.

Without Energy Transfer between Excited States of N

In these two papers we have shown that without taking into account the energy transfer between the excited states, the values of the collision integrals obtained through the known interaction potential are quite the same. The values of averaged collision integrals $\bar{Q}_{SD}^{(\ell,s)}$, $\bar{Q}_{SP}^{(\ell,s)}$, $\bar{Q}_{DD}^{(\ell,s)}$, $\bar{Q}_{DP}^{(\ell,s)}$ and $\bar{Q}_{PP}^{(\ell,s)}$ are slightly greater than $\bar{Q}_{SS}^{(\ell,)}$. It can be noted that the collision integrals of two nitrogen atoms in the excited ^{2}D–^{2}D states ($H^3\Phi_u$) or ^{2}D–^{4}S states ($C^3\pi_u$) are lower than the corresponding interaction of two nitrogen atoms in the ground state ($X^1\Sigma_g^+$). This behaviour can be considered as unusual, because atoms in the excited states are commonly regarded as having collision integral with values greater those in the ground state [22]. In this case, independent of chosen transport property, the values obtained classically ($\bar{Q}_{SS}^{(\ell,s)}$) are overestimated of only few percents (at most 3%) in comparison to those obtained by taking into account the excited states.

Generally:

- The number of repulsive potentials is larger than that of attractive potentials and their total statistical weights are always larger (as example for the interaction C–O we have eight attractive potentials (total statistical weight 24) and 10 repulsive potentials (total statistical weight 56)) [11],
- The data is more easily available for attractive potential, as these corresponding states can be studied by optic spectroscopy. This remark is confirmed by the previous table.

Therefore the collision integrals that we used in our calculation are overestimated (except for the $N(^4S)$–$N(^4S)$ interaction), principally for the $N(^2D)$–$N(^2D)$ collision, leading to an underestimation of the different transport properties.

From above it can be concluded that in given case the classical approach is applicable.

With Energy Transfer between Excited States of N

The introduction of the energy transfer between the different states of N has only a small influence on the values of viscosity and translational thermal conductivity (see Figs. 4 and 5 part I) but also on electrical conductivity (this transport property is strongly related to electronic density). The maximum relative discrepancy $D_M(\%)$ between the total thermal conductivities determined with the first (five species) and the second (eight species) approaches is around 10% for all pressure values. It is due to the fact that calculation method of k_{int} depends only on $\bar{Q}_{SS}^{(\ell,s)}$ and k_{reac} depends on energy transfer (the values of the collision integrals are large for $\ell = 1$ or 3) for atomic nitrogen and as shown in Table 5 of part I. This discrepancy is obtained for T = 9,500 K and 11,000 K at p = 1 and 10 atm when the values of k_{tot} are minimum.

To minimize $D_M(\%)$ we have replaced $\bar{Q}^{(\ell,s)}$ by weighted mean cross sections $\bar{Q}_f^{(\ell,s)}$ (relation [8] of part I) which is function of $\bar{Q}^{(\ell,s)} \ldots \bar{Q}^{(\ell,s)}$. The introduction of these cross sections reduces $D_M(\%)$ from 10% to 5%.

It should be kept in mind that there are two approaches for taking into account the excited N states:

(a) Classically using k_{int}
(b) By determining k_{reac} using following successive reactions (the densities of $N(^2P)$ and N(R) are always negligible: Figs. 1 and 2):

$$N_2 \rightarrow 2N(^4S)$$
$$N(^4S) \rightarrow N(^2D).$$

If $\bar{Q}_{SS}^{(\ell,s)} = \bar{Q}_{SD}^{(\ell,s)}$ then $k = k_{reac}$. In our case, the ''exact'' value of the thermal conductivity (taking into account energy transfer) is between $k_{tot} = k_{tr} + k_{reac} + k_{int}$ and $k_1 = k_{tr} + k_{reac}$. This remark can be generalized for all the plasma chemical mixtures used in the study. However, we have $\bar{Q}^{(\ell,s)}$ and this relation $\bar{Q}_{ij}^{1,1}(T) >> \bar{Q}_{ii}^{(1,1)}$ is also always true. The ratio $A = \bar{Q}_{ij}^{(1,1)}(T)/\bar{Q}_{ii}^{(1,1)}$ and the values of A are generally between 2 and 4. For atomic nitrogen we have A = 3 and for atomic oxygen we have at 10,000 K[22] $\bar{Q}^{(1,1)} = 9.7$ Å^2, $\bar{Q}_{PD}^{(1,1)}(T) = 21.9$ Å^2 and $\bar{Q}_{PS}^{(1,1)}(T) = 19.5$ Å^2 leading to A = 2.3 and 2.0 respectively.

In Fig. 9 we represent the evolution of the total conductivity versus temperature at p = 1 atm. The total conductivity is calculated classically (k_{tot} (SS)) or taking excited states (k_{tot} (SDPR)) into account along with k_1 (SS) =k_{tot} (SS)–k_{int} and k_2 (SS) =k_{tot} (SS)–2 k_{int} / 3. For k_2 we used a weight of 2 / 3 for k_{int} based on the values of two collision integrals $\bar{Q}_{SD}^{(1,1)}(T) \approx 3\bar{Q}_{SS}^{(1,1)}$ in this temperature range.

It should be noted that k_{tot} (SDPR) $\approx$ k_2 (SS) but this result may be obtained only after calculation of $\bar{Q}_{SD}^{(\ell,s)} \ldots$

In our opinion we have two methods to determine the transport properties in plasma.

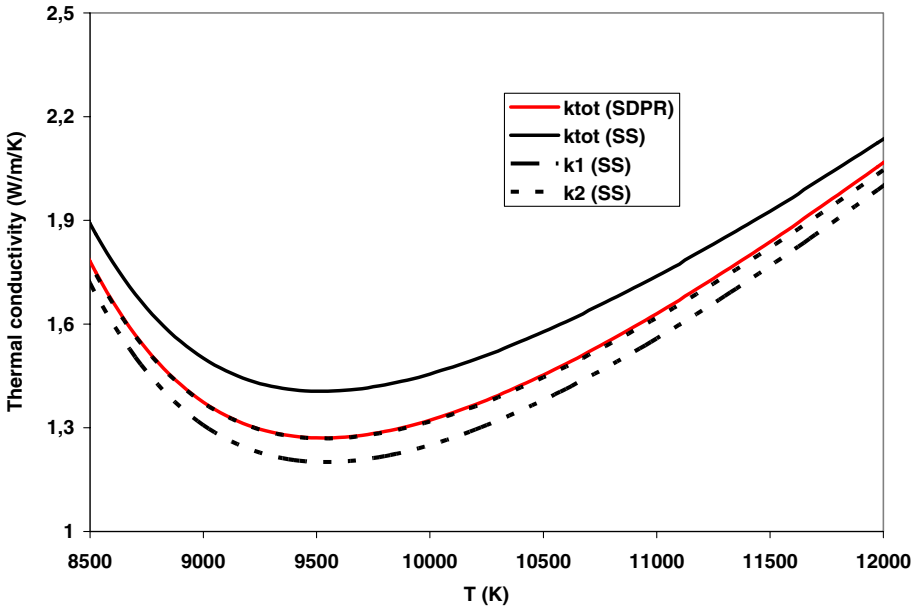

Fig. 9 Evolution of thermal conductivities for $p = 1$ atm

- The first one is the classical well known approach in which some elementary approximation (see previous remark) may be done to increase the accuracy of the transport properties. While we take into account the energy transfer in molecules or atoms, the values of these transport coefficients become smaller. For $p \approx 1$ atm, the classical approach is sufficient.
- In this study, we have introduced energy transfer only between the excited states of N but we have not taken into account the charge transfer as, for example, in the following reaction:

$$N(^2D) + N^+(^3P) \rightarrow N^+(^3P) + N(^2D)$$

The composition may be determined by a state-to-state approach. In the simple case of hydrogen plasma (H^+ can be only in a ground state) Capitelli et al. [3, 5] calculated the composition taking into account the different states of H (up to $n = 12$). Then they estimated the charge transfer (H(n)–H^+) and excitation transfer (H(n)–H(m)) cross sections and they showed that this kind of reaction leads to a non-negligible difference between transport properties calculated with ''usual'' and ''abnormal'' cross sections (Capitelli notations). This kind of approach may be essential at high pressure: at 100 atm, Capitelli [3] obtained discrepancies between the values of ''usual'' and ''abnormal'' transport properties up to 70%. Even if it is possible to apply a state-to-state theory on hydrogen plasmas, for other cases the greatest problem of this method is the number of electronic states and lack of available data (unknown potentials). However works are developed to take into account excited and charge transfers involving excited states of atoms and ions. As an example and in the nitrogen case, Kosarim et al. [23] study the resonant charge transfer between the $N(^4S, ^2D, ^2P)$ and $N^+(^3P, ^1D, ^1S)$.

References

1. Boulos MI, Fauchais P, Pfender E (1994) Themal plasmas fundamentals and applications. Plenum Press, New York
2. Murphy AB, Arundell CJ (1994) Plasma Chem Plasma Process 14(4):451
3. Capitelli M, Celiberto R, Gorse C, Laricchiuta A, Pagano D, Traversa P (2004) Phys Rev E 69:026412
4. Capitelli M, Laricchiuta A, Pagano D, Traversa P (2003) Chem Phys Lett 379:490
5. Capitelli M, Celiberto R, Gorse C, Laricchiuta A, Minelli P, Pagano D (2002) Phys Rev E 66:016403
6. Eletskii AV, Capitelli M, Celiberto R, Laricchiuta A (2004) Phys Rev A 69:042718
7. White WB, Dantzig GB, Johnson SM (1958) J Chem Phys 28:751
8. Rat V, André P, Aubreton J, Elchinger MF, Fauchais P, Lefort A (2001) Phys Rev E 64:026409
9. Rat V, André P, Aubreton J, Elchinger MF, Fauchais P, Vacher D (2002) J Phys D 35:981
10. Rat V, André P, Aubreton J, Elchinger MF, Fauchais P, Lefort A (2002) Plasma Chem Plasma Process 22:475
11. Sourd B, Aubreton J, Elchinger MF, Labrot M, Michon U (2006) J Phys D 39:1105
12. Sourd B, André P, Aubreton J, Elchinger M-F (2007) PCPP 27(1):35
13. Champagne HH, Li X, Hunt KLC (2000) J Chem Phys 112(4):2893
14. Stallcop JR, Partridge H, Levin E (2000) Phys Rev A 62, 062709(1–15)
15. Stallcop JR, Partridge H, (1997) Chem Phys Lett 281:212
16. Stallcop JR, Partridge H, Levin E (2001) Phys Rev A 64(4), 042722(12)
17. Sun W, Morrison MA, Isaacs WA, Trail WK, Alle DT, Gulley RJ, Brennan MJ, Buckman SJ (1995) Phys Rev A 52(2):1229
18. Phelps AV, Pitchford LC (1985) Phys Rev A 31(5):2932
19. Shyn TW, Carignan GR (1980) Phys Rev A 22(3):923
20. Mi L, Bonham RA (1998) J Chem Phys 108(5):1904
21. Hirschfelder JO, Curtiss CF, Bryon R (1954) Molecular theory of gases and liquids. John Wiley Sons, Inc.
22. Capitelli M, Ficocelli EV (1972) J Phys B 5:2066
23. Kosarim AV, Smirnov BM, Capitelli M, Celiberto R, Laricchiuta A (2006) Phys Rev A 74:062707